Md. Alamgir[1]

Engineer,
General Electric Co.,
San Jose, Calif. 95125

C. Y. Kan[1]

Engineer,
Nutech,
San Jose, Calif. 95119
Assoc. Mem. ASME

J. H. Lienhard[1]

Professor,
Department of Mechanical Engineering,
University of Houston,
Houston, Tex 77004
Fellow ASME

An Experimental Study of the Rapid Depressurization of Hot Water[2]

New measurements of the pressure history in 5.08 and 1.27 cm i.d. tubes during extremely rapid depressurization from BWR and PWR conditions are presented. The pressure to which the present system (as well as the systems of other investigators) returns, is successfully correlated using a suggestion by Stuhmiller. New pressure undershoot data are given here, but they are rationalized elsewhere. The rate of opening, and the rarefaction wave speed, in the present system are also presented and correlated. The present study suggests that scaled replications of the early process of depressurization are reliable.

Introduction

The problem of insuring that the design of nuclear reactors is safe has led to the need for a variety of fundamental experiments. One such safety problem is that of knowing exactly what behavior would follow a guillotine break of a major BWR or PWR recirculation pipe, both from the standpoint of rate-of-loss of cooling water, and from the standpoint of the structural loads that it could impose. Data obtained in a fundamental experiment that reduces this kind of break to its most elementary form, namely the very sudden opening of a straight horizontal pipe containing hot water at BWR or PWR conditions, have helped us to understand how a system might react to such a break.

Experimental results of this kind have been obtained by Edwards and O'Brien [1], Bogartz, et al. [2–4], Rassokhin, et al. [5], Gallagher [6], Brockett, et al. [7], Allemann, et al. [8], Sozzi and Fedrick [9], and Lienhard, et al. [10]. The prediction of the behavior following such a break in a pipe is called the "Standard Problem 1."

All prior tests, except our own [10], used burst-diaphragm techniques that yielded rates of depressurization equal to or less than about 0.75 Matm/s. Our experiments involved the very rapid depressurization of water from pressures as high as 153 atm (2250 psia) and temperatures as high as 321°C, in a 1.27 cm i.d. tube. With the aid of a recently-patented opening device [11][3] we achieved depressurization rates as high as 1.8 Matm/s with correspondingly higher pressure undershoots than previous investigators reached.

Our objective in this paper is to present observations similar to those presented in [10], but to include data for a much larger tube than was used previously (5.08 cm i.d. or 16 times the cross-sectional area). With these data and those of previous investigators we shall:

• Develop a correlation of pressure undershoot which represents all previous and present data (This is done elsewhere in this journal [12].),

• Develop a general correlation of the quasi-static pressure to which the water first returns after pressure undershoot,

• Arrive at some general conclusions about the role of geometric scale and water purity upon the performance of such experiments or prototype behavior.

Experiment

Figure 1 is a schematic diagram of the 5.08 cm i.d. tube. It consists of an 11 m long stainless steel (ASTM A213) pipe connected to a 0.2 m stainless steel block, bored to match the pipe. The first 2.32 m of pipe behind the block is the heated test section; the rest of the pipe is simply present to delay the return of reflection of the rarefaction

wave to the test section for about 13 ms after the pipe is opened.

The POP the QORC opening mechanism was incorporated into the front block as shown in Fig. 2. This is a fairly direct adaptation of the 1.27 cm dia pipe opening mechanism described more fully in [10, 11, 13, and 14]. But the structural design in this case had to be based on forces 16 times larger than in the previous design. It was arranged as follows.

The discharge end of the pipe was sealed with a disk-shaped plug and an O-ring. The plugs were made of mild steel or titanium. Silicon O-rings were used for temperatures up to 250°C. For higher temperature Kalrez O-rings were employed. Two titanium arms (see Fig. 2) secured the plug over the open end of the tube. A pair of L-shaped brackets were fastened to the front end on each side of the block. A common hinge pin passed through these two brackets and the arm. Each arm could be swung in and out of position about its hinge. This arrangement largely eliminated thermal-expansion-related binding between the contact surface of the plug and the arms. A weighted main cam guided on two vertical shafts was dropped from a height of 3.65 m, using a manual remote control. The falling main-cam engages a mating cam on each arm and drives them apart to release the edges of the plug. The plug is then forced out by the higher internal liquid pressure and depressurization ensues.

The test section was heated with semi-cylindrical strip heaters fitted on the outside of the pipe. To offset large vertical temperature differences resulting from natural convection only the bottom-half of the test section was heated. At a given location the water temperatures at the top, bottom and side of the pipe could generally be maintained within 5°C of each other.

Figure 3 shows the location of the pressure transducers (PT-) and the thermocouples (TC-) in the test section. In the present test, a Sundstrand 601B1 water-cooled quartz pressure transducer was mounted flush with the pipe i.d. at each of the locations PT-1 and PT-3. Transient pressure signals during depressurization, were transmitted to and stored on a pair of Tektronix 7613 storage oscilloscopes through a pair of dual mode charge amplifiers. The oscilloscopes were triggered by an external battery circuit about 3 to 5 ms prior to depressurization. A total of 11 grounded-junction sheathed chromel-alumel thermocouples were located at top, bottom, and sides of the pipe, and were connected to a common digital temperature readout device that could be read accurately within 0.6°C

The test preparation proceeded as follows: the discharge end of the pipe was sealed using the plug and the arm, and the falling weight was positioned at its upper level. The pipe was evacuated to a pressure of about 0.05 atm using the vacuum pump. The pipe was then filled with double distilled water that had been degassed by boiling for about an hour. All the valves were closed and the system was cold-tested at high pressure for possible leaks. Next the test section heaters were switched on. While the water was being heated the system pressure, read from a standard Bourdon gage (accuracy ± 2 psi), was maintained 20 to 30 atm above the saturation pressure at the current water temperature. For a typical hot water test the heating duration was about 3 to 5 hr. When the desired temperature and pressure were reached the heaters

---
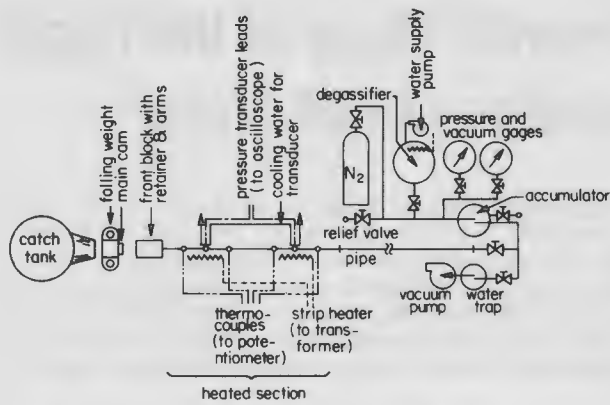
Fig. 1 Layout of apparatus for 5.08 cm i.d. pipe experiment

were switched off and some time (usually 30 s) was allowed for reversal of heat flow direction. Finally, the falling weight was released by remote control. The depressurization began as the plug was released and the transient pressure history at the PT locations was stored on the oscilloscope screen during the first 20 ms or so. These traces were subsequently photographed.

The data reported in this paper also include some new results obtained in the older 1.27 cm i.d. apparatus. Since these experiments and their accuracy are described in detail by Alamgir [14] and in references [10] and [13], we simply present the results here without further comment.

Results and Discussion

Results. The initiation of depressurization is accompanied with the generation of a rarefaction wave that propagates away from the pipe-break location into the high pressure liquid. At any axial location of the pipe, the pressure starts to change upon the arrival of this wave. Figure 4 is a representative selection of pressure-time histories in the 5.08 cm i.d. pipe for the two transducer locations PT-1 and PT-3. Included alongside the traces are the pressure and temperature of the water just prior to decompression. The latter temperature was linearly interpolated between the adjacent thermocouples.

The pressure transients show some characteristic features that have already been displayed in [10] and [13]: As the retainers move across the plug faces the pressure drops a little and rather slowly. Once the plug edges are cleared the pressure falls with great rapidity, almost linearly with time, to well below the saturation pressure. This rapid depressurization rate, designated as Σ matm/s, is either totally halted or else greatly attenuated as a result of bubble nucleation. The drop of pressure below p_{sat}, which we call the *pressure undershoot*, has been correlated [12] as a function of the initial water temperature and the depressurization rate in the superheated liquid, Σ'.

Following the pressure undershoot, bubble growth causes the pressure to recover, in most cases nearly exponentially with time, to a quasi-static level $p_{qs} < p_{sat}$. This happens within a few milliseconds of the undershoot and the level persists for 20 ms or longer. In the present 5.08 cm i.d. pipe experiments with hot water, the pressure
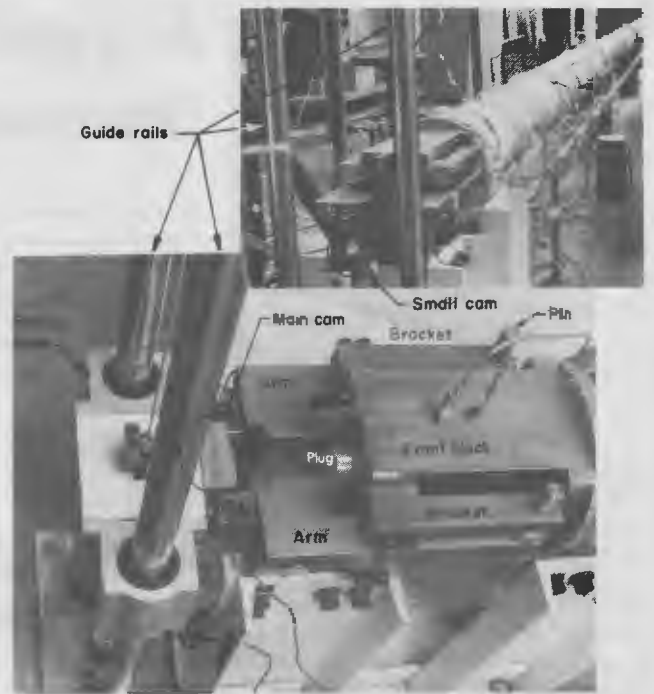
Fig. 2 Front block with plug release mechanism. Inset shows release configuration in relation to entire apparatus.
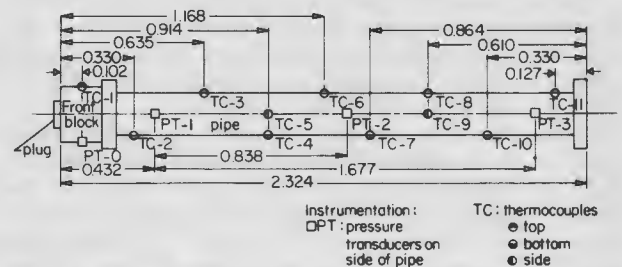
Fig. 3 Locations of thermocouples and pressure transducers in the heated section of the pipe (All dimensions are in meters.)

traces do not show any sign of the return of the reflected rarefaction wave since we used a long pipe.

Table 1 lists the initial test conditions, the measured Σ and Σ', the measured nucleation or minimum pressure and the rarefaction speed for various runs.[3] The measured values of Σ and Σ' were fairly close to one another in the 5.08 cm i.d. pipe tests. Table 2 gives new test data[3] obtained in the 1.27 cm pipe.

The Rate of Depressurization, Σ. The rate of depressurization is a representation of how fast a break area is created or how quickly

---

[3] Estimated accuracies for the original and reduced data are, for Σ and Σ': ±15 percent, all pressures: ±2 percent of p_i, all temperatures: ±0.6°C.

───Nomenclature───

c = speed of sound in water
c_{pf} = specific heat of water
D = pipe or tube diameter
h_{fg} = latent heat of vaporization of water
Ja_{qs} = a Jakob number defined in equation (5)
m = mass of plug divided by cross-sectional area of pipe
$p, p_i, p_n, p_{qs}, p_{sat}$ = pressure, initial system pressure prior to depressurization, local minimum pressure reached by system im-

mediately following depressurization, quasi-static pressure to which system momentarily recovers following depressurization, saturation pressure at T_i.
R = radius of a bubble
T, T_i, T_{qs} = temperature, initial system temperature, temperature at p_{qs}
t = time
$V_{eff} = \kappa c p_i$
v = specific volume

$v_p = \kappa c (p_i - p)$
δ = effective thickness of cooled layer around a growing vapor bubble
κ = isothermal compressibility of water
ν = kinematic viscosity of water
ρ, ρ_f, ρ_g = density, density of liquid, density of vapor
Σ, Σ' = the approximately constant rate of depressurization from p_i to p_n, Σ evaluated between p_{sat} and p_n
$\tau = m \kappa c$
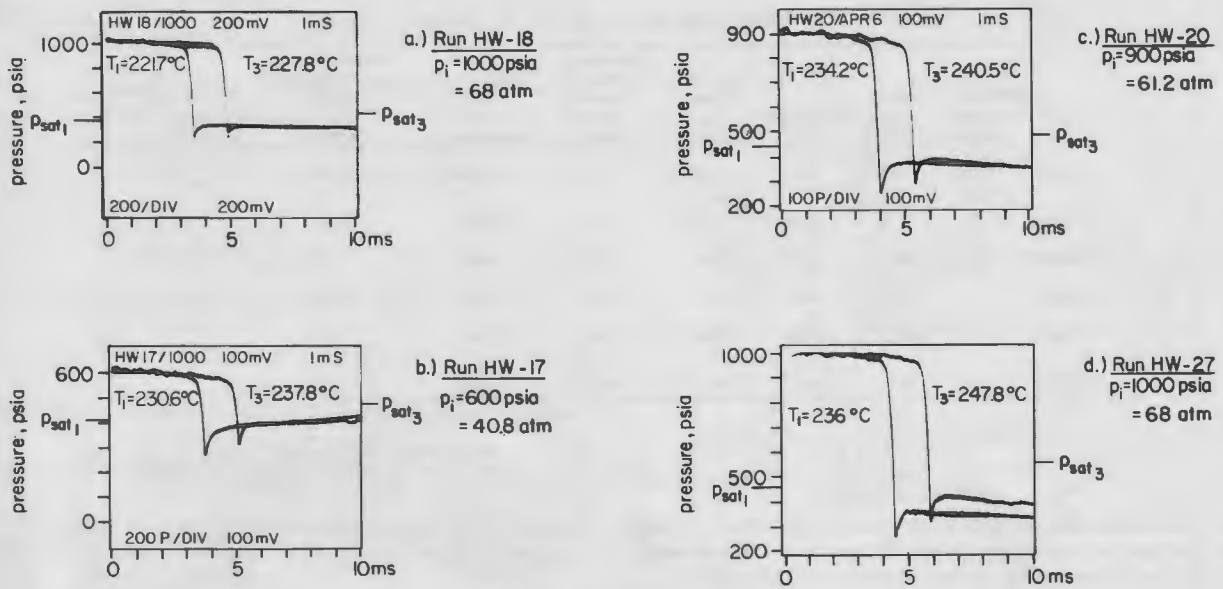
Fig. 4   Pressure-time histories at PT-1 (left trace) and PT-3 (right trace) locations in the 5.08 cm i.d. pipe

Table 1   Experimental results for the 5.08 cm i.d. pipe

Run No.	Pressure p_i (atm)	Interpolated Temperatures T_i		Saturation Pressure P_{sat}		Minimum or Nucleation Pressure p_n		Overall Depressurization Rate Σ		Depressurization Rate in Superheated Water Σ'		Measured Rarefaction Speed C (m/sec)	Plug Mass Per Unit Area m (gm/cm²)	Water Condition
		PT-1 (°C)	PT-3 (°C)	PT-1 (atm)	PT-3 (atm)	PT-1 (atm)	PT-3 (atm)	PT-1 (Matm/sec)	PT-3 (Matm/sec)	PT-1 (Matm/sec)	PT-3 (Matm/sec)			
CW-01	17	21	21	0.024	0.024	2.38	1	0.017	0.02	–	–	1448	12.38	Unboiled, distilled
CW-02	34	21	21	0.024	0.024	5.1	1	0.061	0.065	–	–	1505	12.38	Boiled, distilled
CW-04	6.8	22	22	0.027	0.027	1.63	2.31	0.0014	–	–	–	1450	13.57	Unboiled, distilled
HW-01	17	141	154	3.674	5.307	2.72	4.01	0.048	0.046	0.077	0.075	1500	12.38	Boiled tap water
HW-21	3.4	117.2	121.7	1.793	2.066	1.5	1.84	0.002	0.00028	0.002	0.00028	–	13.43	Boiled, distilled
HW-26	7.15	135	140.6	3.089	3.623	2.25	3	0.0067	0.0056	0.0067	0.0056	1449	13.43	"
HW-24	6.12	140.6	145.6	3.623	4.164	2.96	3.47	0.005	0.0058	0.01	0.0037	1480	13.57	"
HW-22	10.2	144.4	153.1	4.04	5.13	3.40	4.15	0.0136	0.0147	0.023	0.0147	1463	13.43	"
HW-23	10.9	148.6	157.8	4.55	5.76	3.54	4.63	0.0194	0.0167	0.0234	0.018	1429	13.43	"
HW-13	58	167.2	169.4	7.35	7.69	4.63	4.7	0.032	0.033	0.032	0.033	1430	13.57	"
HW-15	68	201.7	208.3	15.87	17.83	10.21	11.57	0.211	0.195	0.227	0.199	1327	13.57	"
HW-10	68	215.6	216.7	21.03	21.43	12.59	17.28	0.212	0.204	0.212	0.209	1256	12.38	Unboiled, distilled
HW-18	68	221.7	227.8	23.54	26.54	15.11	15.99	0.220	0.224	0.196	0.203	1255	13.43	"
HW-16	68	226.7	234.4	26	29.94	16.47	17.69	0.259	0.255	0.259	0.255	1245	13.57	"
HW-25	40.83	228.9	234.4	27.05	29.94	18.03	19.39	0.156	0.135	0.156	0.135	1188	13.43	Boiled, distilled
HW-17	40.83	230.6	237.8	27.76	31.78	19.05	22.11	0.099	0.098	0.099	0.098	1245	13.43	"
HW-20	61.24	234.2	240.6	29.76	33.34	17.69	20.41	0.170	0.176	0.170	0.176	1217	13.43	"
HW-27	68	236.1	247.8	30.84	37.80	18.17	22.6	0.189	0.182	0.189	0.182	1189	13.88	"
HW-14	68	251.7	257.2	40.35	44.23	27.22	30.62	0.186	0.18	0.199	0.193	1191	13.57	"
HW-12	68	253.3	257.2	41.51	44.23	–	31.30	–	0.133	–	0.133	–	12.38	"
HW-19	102	–	239.4	–	33.07	–	20.41	–	0.3	–	0.314	–	13.43	"
HW-07	57.15	211.1	221.1	19.19	23.34	12.25	15.31	0.245	0.251	0.245	0.251	1311	7.03	"
HW-30	63.96	251.9	258.9	41.51	45.50	28.78	30.62	0.136	0.143	0.136	0.156	1159	13.57	"

the high pressure liquid is allowed to expand. The magnitude of Σ thus depends on the extent of inertia associated with the break that the expanding liquid has to overcome. For our experiments, a dynamic force balance between the moving plug and rarefied liquid behind it yielded[4] (see [10])

$$\frac{dp}{dt} = -\frac{p}{\tau} \tag{1}$$

where the velocity of the expanding liquid (which also equals that of the plug) is $v_p = \kappa c(p_i - p)$ and $\tau \equiv m\kappa c$. A characteristic depressurization rate, $p_i/m\kappa c$, and an effective liquid velocity, $V_{eff} = \kappa c p_i$, can then be identified as parameters that govern Σ. In the preceding one-dimensional considerations we have ignored the liquid viscosity and the size of the system.

When these system variables are used, we may write the functional form for Σ as

---

[4] Certain undefined terms in this section are defined in the Nomenclature. In [10], equation (1) had an area-ratio factor that would arise if the liquid jet immediately expanded to the plug diameter. Recent photographic evidence suggests that this expansion does not occur.

Table 2 New data for the 1.27 cm I.d. Pipe

Run No.	Pressure Transducer Location	Pressure p_i (atm)	Temperature (°C)	Saturation Pressure p_{sat} (atm)	Minimum or Nucleation Pressure p_n (atm)	Overall Depressurization Rate Σ (Matm/sec)	Depressurization Rate in Superheated Water Σ' (Matm/sec)	Water Condition
AHW07	PT-1*	6.46	137.2	3.295	2.729	0.0075	0.0079	distilled and boiled
AHW06.		7.14	129.4	2.622	2.177	0.0067	0.007	"
AHW08		49.3	223.9	24.65	11.57	0.331	0.348	"
AHW05		65.3	264.4	49.77	23.14	0.492	0.517	"
AHW04	PT-2	68	232.8	29.04	17.69	0.258	0.272	distilled but unboiled
AHW03	PT-2	68	260	46.33	29.26	0.363	0.375	"

$$\Sigma = fn\left[\frac{p_i}{m\kappa c}, V_{\text{eff}}, \nu, D\right] \qquad (2)$$

where ν is the kinematic viscosity of water and D, the pipe i.d., is used as the characteristic size of the system. Dimensional analysis results in two dimensionless groups consistent with the Pi-Theorem.

$$\frac{\Sigma m\kappa c}{p_i} = fn\left(\frac{V_{\text{eff}}D}{\nu}\right) \qquad (3)$$

where the group $\kappa c p_i D/\nu$ may be called a depressurization "Reynolds number". The isothermal compressibility of water $\kappa \equiv -(1/\upsilon)(\partial\upsilon/\partial p)_T$ has been calculated[5] from the equation of state for water given by the 1967 E.R.A. Steam Tables [15] and is presented in Fig. 5.

Figure 6 shows that the nondimensional depressurization rate, $\Sigma m\kappa c/p_i$, in all of our tests increases monotonically with $V_{\text{eff}}D/\nu$. The overall behavior of the data supports the validity of equation (3). The maximum value of the ordinate in the figure is given by equation (1) as unity. The (+) symbols are for certain 1.27 cm i.d. pipe tests with a slit or orifice constriction in the pipe. For these data the Reynolds number was based on either the orifice diameter (0.52 cm) or square-root of the slit area (0.45 cm). Ninety percent of all data lie within ±30 percent of the faired curve.

Speed of the Rarefaction Wave. In pipe decompression experiments the rarefaction speed can exceed the speed of sound in the liquid as the result of bonding between the liquid and the steel pipe wall. Evidence of this fact was provided by the measured rarefaction speed in our 1.27 cm i.d. pipe tests [10]. 5.08 cm pipe rarefaction speed data, shown in Fig. 7, also indicate a similar trend, but the speed augmentation is less because the ratio of the theoretical mean sound speeds for the two pipes (see equation (5) of [10]) is $\bar{c}_{5.08}/\bar{c}_{1.27} = 0.975$.

Quasi-Static Pressure Recovery Following the Pressure Undershoot. We have noted that the system pressure recovers to a quasi-static level, a few milliseconds after the plug is released. This pressure is less than p_{sat} at the initial water temperature. The time dependence of this recovery process appears to be related to bubble growth rate in the associated variable pressure field and to the gross liquid motion around the location of interest. However, for the purpose of predicting the recovery pressure level, p_{qs}, we use the following idealized model, developed by modifying a similar analysis by Stuhmiller [16].

Stuhmiller considered a growing vapor bubble of radius R with the vapor saturated at the current liquid pressure. The thermal energy required to grow this bubble is provided by cooling of a thin liquid layer around the interface. Instead of accepting Stuhmiller's suggestion that a lump-cooling of this layer takes place, we consider the existence of a time-dependent temperature profile in this developing thermal layer. We define $T_{qs} \equiv T_{sat}(p_{qs})$ and observe that the temperature increases asymptotically from this value to T_i with x, the radial distance from the bubble interface. Thus
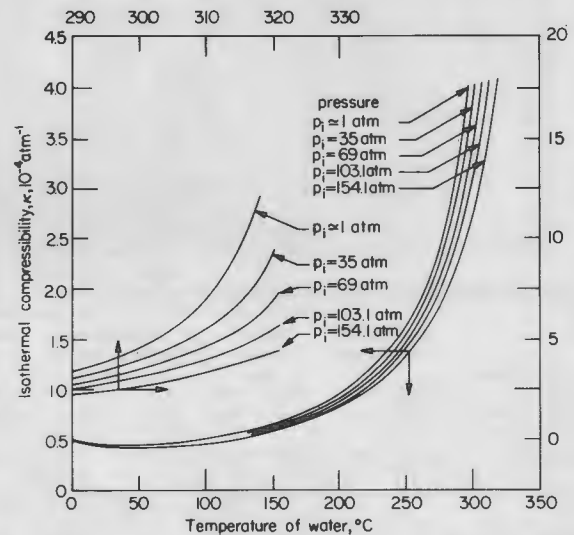
Fig. 5 The isothermal compressibility of subcooled and moderately superheated water
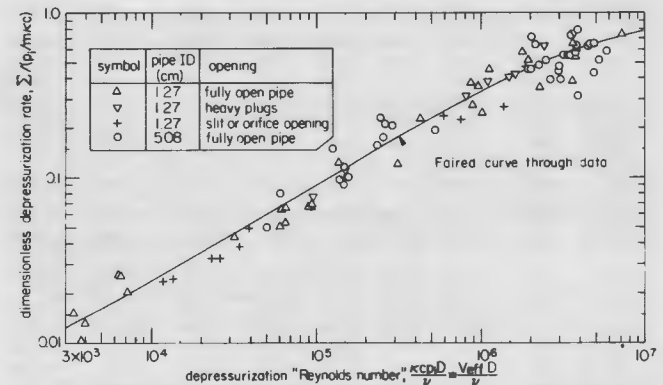
Fig. 6 Correlation of all opening-rate data for both pipes using the POP the QORC device
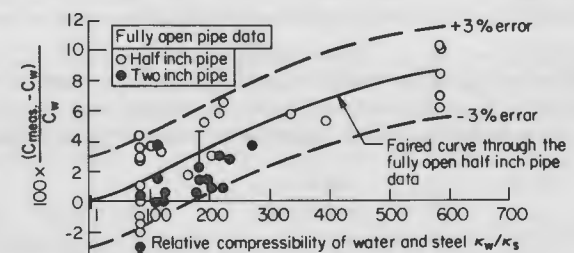
Fig. 7 Deviation of measured rarefaction speed from the calculated sound speed

$$\frac{4}{3}\pi R^3 \rho_g h_{fg} = 4\pi R^2 \rho_f c_{pf} \int_0^\infty (T_i - T)dx \qquad (4)$$

where ρ_f, ρ_g, c_{pf} and h_{fg} are the saturated liquid and vapor densities, the liquid specific heat, and the latent heat of vaporization, all evaluated at T_i. Drawing an analogy with the displacement thickness in a hydrodynamic boundary layer, we introduce an energy thickness, δ, defined as

$$\delta(T_i - T_{qs}) = \int_0^\infty (T_i - T)dx \qquad (5)$$

Combining equation (5) with equation (4), we get

$$\frac{4}{3}\pi R^3 \rho_g h_{fg} = 4\pi R^2 \rho_f c_{pf} \delta(T_i - T_{qs}) \qquad (6)$$

Equation (6) can be rewritten to give a volumetric Jakob number

$$\text{Ja}_{qs} \equiv \frac{\rho_f c_{pf}(T_i - T_{qs})}{\rho_g h_{fg}} = \frac{1}{3}\frac{R}{\delta} \qquad (7)$$

The temperature T_{qs} can be calculated from equation (7) if we know the ratio of the bubble radius R to the equivalent thickness, δ, at p_{qs}.

The liquid around the growing bubble interface is not stationary, but agitated, as a result of instabilities that arise when a less dense vapor is accelerated into a dense liquid. Stuhmiller invoked a turbulent diffusivity argument and obtained $\delta/R \simeq 0.265$. If we accept this value we get a constant value of Ja_{qs} from equation (7)

$$\text{Ja}_{qs} = \frac{\rho_f c_{pf}(T_i - T_{qs})}{\rho_g h_{fg}} \simeq 1.26 \qquad (8)$$

This result is based on several assumptions and should really only be viewed as a correlation in which 1.26 might be replaced with an adjustable constant. That this constant subsequently turns out to be exactly 1.26, is no doubt fortuitous.

Equation (8) immediately allows us to evaluate the recovery pressure level, p_{qs}, as p_{sat} at T_{qs}, once the initial water temperature T_i is known. Figure 8 shows the variation of the predicted p_{qs} with T_i for water as the solid curve, with ρ_f, c_{pf}, ρ_g and h_{fg} being evaluated as saturation properties at T_i. The saturation pressure, $p_{sat}(T_i)$, is shown as the dashed curve. Figure 8 verifies an important claim, made previously by Brown [17], that $p_{qs} \neq f_n (\Sigma', p_n,$ or other opening-rate parameters.)

The difference, $p_{sat}(T_i) - p_{qs}$, is a monotonically increasing function of the initial temperature T_i that dwindles to a negligible value only at very low temperatures. Experimental data for p_{qs} from the many available sources have been plotted on the same graph and they show very good agreement with the predicted curve. They match the prediction with an rms deviation of 4.27 percent and maximum deviation of 14 percent.

A point may be made about the data of Sozzi and Fedrick [9], shown by plus symbols. Their depressurization apparatus used a short pipe (3.25 m or 0.56 m) connected to a very large reservoir. In their experiments the pressure first recovered to a plateau below the saturation pressure and then was kicked up above the saturation pressure. We suspect the latter behavior to be the combined result of the presence of the reservoir and the reflected rarefaction wave interacting with the recovering pressure. When these effects are absent, the first pressure plateau, which we have chosen to plot, would represent the true recovery pressure.

Correction of previously Reported 1.27 cm Pipe PT-1 Temperatures. The high temperature blowdown tests with the half-inch pipe were carried out with a water cooled front section of the pipe [10]. This was necessary to avoid the thermal expansion binding between the plug and the retainers. The temperatures at the first transducer (PT-1) location were obtained by extrapolating the thermocouple readings without realizing how abruptly the water-cooling caused the temperature to change, near it. It now appears that the reported PT-1 temperatures were high.

The true local temperature, T_i, for these runs, can be estimated using the measured value of the quasi-static pressure p_{qs} (and hence
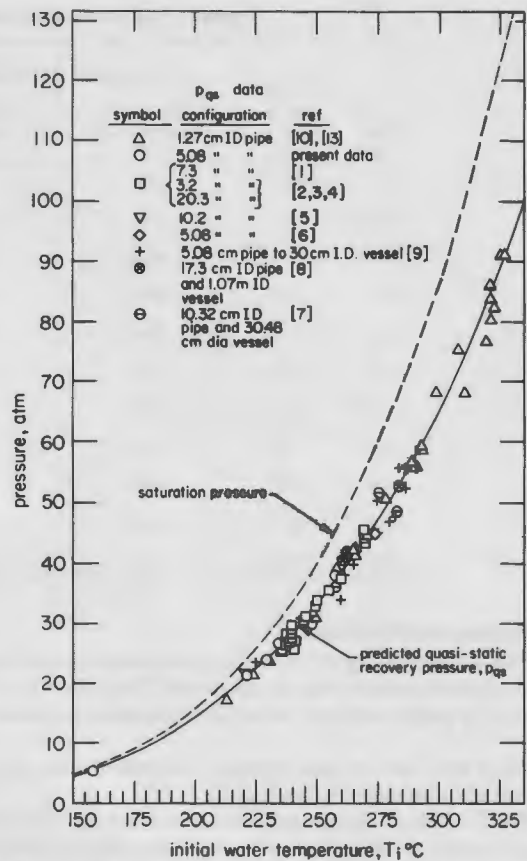
Fig. 8 Comparison of predicted quasi-static recovery pressure with experimental data

$T_{qs} = T_{sat}(p_{qs})$ in equation (8). Table 3 shows the correct temperatures for the eleven tests in question and the magnitude of the errors in the originally measured temperature range from 8.3°C to 17.3°C. These data, of course do not appear in Fig. 8.

The Problem of Dimensional Scale and Water Purity in Reactor Blowdown Experiments. We present correlations of four different dependent variables here and in [12]. These are: (1) pressure undershoot, (2) quasistatic pressure recovery, (3) rarefaction wave speed, and (4) opening rate.

The first two parameters are the most important for the nuclear engineer who is interested in predicting the early blowdown behavior. Data for these parameters, measured over a *256-fold* variation of pipe area, have been correlated without showing any apparent influence of pipe size.

The rarefaction speed can be increased by a few percent of the speed of sound by pipe size, only if the pipe is quite small and thick-walled. The opening rate is a *dependent* variable in our scheme of experimentation, and dimensional scale must be included in its correlation. However, in most nuclear safety analyses it must be specified as an independent variable.

Thus, the present results suggest that reduced-scale modeling is entirely reliable, at least for specifying the primary features of the initial response of hot water to sudden depressurization.

Furthermore, the present experiments include 10 cases in which the water was either undistilled, or unboiled prior to pressurization, or both. These data correlate perfectly well with the other data, some of which reflect different preparation schemes from that which we normally used. Probably the act of bringing water to BWR and PWR conditions constitutes a more significant preparation (in terms of, say, degassing) than anything that can be done at atmospheric pressure. Of course these remarks do not apply if a system is exposed[6] to large amounts of soluble noncondensible gases at p_i.

Table 3 Correction of 11 values of T_i at PT-1 previously reported in [10]

Run No.	Initial Pressure p_i (atm)	Temperature at PT-1 Location T_i		Measured Minimum or Nucleation Pressure p_n (atm)	Overall Rate of Depressurization Σ (Matm/sec)	Rate of Depressurization in Superheated Water Σ' (Matm/sec)
		Previously Reported in [10] (°C)	Corrected Using Equation (6) (°C)			
51	102	268	256.6	10.2	1.36	1.65
45	102	271	262.9	10.2	1.12	1.35
42	144.3	290.6	282.2	25.2	1.18	1.48
30	153.1	293.3	278.1	29.3	1.05	1.05
50	153.1	293.3	281.1	20.4	1.49	1.74
44	153.1	293.3	282.8	27.9	1.41.	1.41
64	153.1	296	287.2	26.5	1.62	1.62
4-HV	68	231.1	215	12.9	0.15	0.12
2-H	102	262.8	246.1	23.1	0.19	0.21
5-HV	102	263.3	246.1	20.3	0.54	0.54
3-H	129.3	302.2	287	42.2	0.3	0.3

Conclusions and Summary

1 New data that bring the element of dimensional scale into the present experimental program are presented. They show the initial response of a pressurized hot water pipe to sudden depressurization.

2 These data include new pressure undershoot data that are correlated in a companion paper [12].

3 The data show that after pressure undershoot, the system pressure recovers to within about 4.2 percent of a sub-saturated value which corresponds to T_{qs} as correlated by equation (8).

4 The most important aspects of system response following sudden depressurization appear not to be influenced by dimensional scale, even when the pipe is as small as 1.27 cm i.d.

5 No perceptible influence of water preparation upon system response has been revealed by these tests.

6 The rarefaction wave speed is very slightly increased by the pipe walls. This increase is consistent with our discussion of such behavior in [10].

7 The opening rate in experiments such as these can be predicted within ±30 percent by the correlation in Fig. 6.

References

1 Edwards, A. R., and O'Brien, T. P., *Journal of the British Nuclear Energy Society,* Vol. 9, 1970, p. 125.

2 Borgartz, B. O., Goodman, R. M. E., O'Brien, T. P., Rawlingson, M., and Edwards, A. R., "Depressurization Studies, Phase 2: Results of Tests 115 and 130," UKAEA Report SRD-R-115, 1978.

3 Ibid, "Depressurization Studies, Phase 3: Results of Tests 144 and 145," UKAEA Report SRD-R-77, 1977.

4 Ibid, "Depressurization Studies, Phase 3: Results of Tests 142 and 143," UKAEA Report SRD-R-76, 1977.

5 Rassokhin, N. G., Kuzevanov, V. S., Tsiklauri, G. V., Marinchek, Z., and Sella, J., "Critical Conditions with Unsteady Outflow of a Two-Phase Medium with a Pipeline Break," *Teplofizika Vysokikh Temperatur,* Vol. 15, No. 3, 1977, p. 589.

6 Gallagher, E. V., "Water Decompression Analysis for Blowdown of Nuclear Reactors," IITRI-578, IIT Research Institute, Chicago, 1970.

7 Brockett, G. F., Curet, H. D., and Heiselmann, H. W., "Experimental Investigations of Reactor System Blowdown," IN-1348, Idaho Nuclear Corporation, 1970.

8 Allemann, R. T., McElfresh, A. J., Neuls, A. S., Townsend, W. C., Wilburn, N. P., and Witherspoon, M. E., 1971a USAEC Report BNWL-1463 and 1971b USAEC Report BNWL-1470.

9 Sozzi, G. L., and Fedrick, N. A., "Decompression Waves in a Pipe and Vessel Containing Subcooled Water at 1000 psi," NEDE-13333, General Electric Company, Mar. 1973.

10 Lienhard, J. H.; Alamgir, Md.; and Trela, M., "Early Response of Hot Water to Sudden Release from High Pressure," ASME JOURNAL OF HEAT TRANSFER, Vol. 100, 1978, pp. 473–479.

11 Lienhard, J. H., and Borkar, G. S., "Quick Opening Pressure Release Device and Method," U.S. Patent No. 4, 154, 361, May 15, 1979.

12 Alamgir, Md., and Lienhard, J. H., "Correlation of Pressure Undershoot During Hot-Water Depressurization," under review.

13 Borkar, G. S., Trela, M., and Lienhard, J. H., "A Rapid Hot-Water Depressurization Experiment," EPRI Report NP-527, Dec. 1977.

14 Alamgir, Md., "Initial Response of Pressurized Hot Water in A Suddenly Opened Pipe," Doctoral dissertation, Univ. of Kentucky, Mechanical Engineering Department, 1979.

15 Electric Research Association, *1967 Steam Tables,* St. Martin's Press, New York, 1967.

16 Stuhmiller, J. H., "The Physical Process in Pipe Blowdown," *Computational Techniques for Non-Equilibrium Two-Phase Phenomena,* (R. W. Lyczkowski and W. Mathers, eds.) National Heat Transfer Conference, Salt Lake City, Utah, 1977.

17 Brown, E. A., "Experiments on the Explosive Decompression of Water," Armour Research Foundation Report ARF 4132-9, Nov. 1959.

---

[6] While our system is pressurized by N_2 at the cold end of the pipe, the pressurizer is too far from the test section to influence it.